Available online at www.sciencedirect.com

ScienceDirect

Energy Procedia 4 (2011) 3965–3972

Energy Procedia

www.elsevier.com/locate/procedia

GHGT-10

Transient Pressure Response of A Gas Reservoir Arising From Supercritical Carbon Dioxide Injection Through a Partially-Penetrating Well: An Analytical Solution

Sumit Mukhopadhyay[a]*, Shaw-Yang Yang[b], and Hund-Der Yeh[c], Jens Birkholzer[a]

[a]*Lawrence Berkeley National Laboratory, One Cyclotron Road, Berkeley, CA 94720, USA*
[b] *Vanung University, Chungli 32061, Taiwan*
[c] National Chiao Tung University, Hsinchu 30010, Taiwan

Abstract

Injecting CO_2 into a subsurface formation causes a buildup of pressure in the vicinity of the injection well. While a large injection rate can reduce the cost associated with injection, an indefinitely large injection rate can result in excessive formation damage. To obtain an optimal injection rate without exceeding the safe pressure limits, one would like to have some knowledge of the transient pressure buildup characteristics resulting from a particular injection rate. Using some simplifying assumptions, we have developed an analytical solution to predict the transient buildup of pressure resulting from injection of supercritical carbon dioxide from a partially penetrating well into a gas reservoir. We use the analytical solution to study pressure transient characteristics for different formation permeabilities and anisotropy ratios.

Keywords: carbon dioxide; sequestration; pressure buildup; supercritical; analytical solution

1. Introduction

Extensive research [1] is currently being carried out to better understand CO_2 storage in subsurface formations including natural gas reservoirs [2-5]. While this research has helped to address many unresolved issues, many still remain unanswered. In this paper, our objective is to address one of these unresolved issues – the spread of the injected CO_2 in the reservoir and the rise in reservoir pressure immediately after injection of CO_2.

* Corresponding author. Tel: +1-510-495-2440; fax: +1-510-486-5686
E-mail address: Smukhopadhyay@lbl.gov

doi:10.1016/j.egypro.2011.02.336

Injection of CO_2 into deep geological formations is achieved by pumping it down into an injection well. To do so, a pressure differential has to be created between the fluid in the injection well and the formation fluids. A larger pressure differential will clearly force CO_2 more rapidly into the formation, reducing the time needed and cost incurred to complete the injection process. However, increasing the injection pressure can indefinitely increase the pumping cost (affecting the economics of the operation). More seriously, a large, uncontrolled injection pressure can cause serious damage to the storage formation (e.g., through excessive fracturing). To prevent such formation damage, regulatory agencies often restrict the pressure at which fluids can be injected through prescription of safe injection pressures, either at the surface or at the injection point.

Designing an injection system is thus an exercise in optimization. On one side, engineers would prefer to use a large-enough injection rate to reduce time and cost of injection operation. On the other side, they need to ascertain that the injection process will not cause a pressure increase beyond safe limits. To design such an optimal injection process, it is useful to have reliable information about the expected buildup in reservoir pressure (both spatially and temporally) resulting from different applied injection rates. While such information could be obtained from detailed numerical simulations, these simulations require extensive and accurate information about the formation, which often are not available before commencing an injection operation. Performing these numerical simulations is also more cost effective when they are done after the injection process has started, and some reliable insight is already available about formation properties.

In this paper, we offer an analytical solution for predicting the spatial and temporal nature of CO_2 spreading and the pressure buildup resulting from injection of CO_2 into a natural gas reservoir. The analytical solution is not formation specific, and thus is more general in nature than formation-specific empirical relationships. Additionally, because it is developed specifically for carbon dioxide injection, our solution is more appropriate than empirical relationships based on oil and gas operations. On the other hand, any analytical solution, including the one proposed in this paper, is based on certain simplifying assumptions regarding the underlying processes. Consequently, the predictions from an analytical solution are likely to be less accurate than those based on elaborate numerical simulations using extensive site-specific information. However, these analytical solutions often prove useful in providing guidelines, particularly before the start of the actual injection process, when very little about the storage formation has been ascertained.

2. Conceptual Model and Simplifying Assumptions

When CO_2 is injected into the storage formation, different transport mechanisms control its migration. These transport mechanisms may include fluid flow under the pressure gradient created by the injection process, buoyancy caused by density difference between the injected and formation fluids, diffusion, dispersion and fingering, capillarity (resulting from different wetting characteristics of the fluids concerned), dissolution into the formation fluid, mineralization, and adsorption [1].

Some simplifying assumptions are needed so that we can exclude the processes that have either minor effects or are not important for our stated objectives. For example, we can exclude mineralization and adsorption processes because they occur over a long temporal scale, whereas our primary objective is to obtain pressure buildup during or immediately after injection. We also exclude dispersion processes by considering a homogeneous (even though anisotropic) formation.

When CO_2 is injected into saline formations, the large density difference between the resident water and the injected CO_2 creates strong buoyancy forces driving the CO_2 upwards. In a natural gas formation, however, because CO_2 is denser than the natural gas, the injected CO_2 preferentially migrates downwards. In this paper, we exclude buoyancy. While this is expected to introduce some error, the exclusion is likely to produce a conservative estimate of the maximum extent of pressure build up resulting from injection. This is because buoyancy drives fluids away vertically from the point of injection into the formation. Thus, the predicted pressure without buoyancy at the point of injection is larger than the actual pressure (when buoyancy is included). Additionally, when buoyancy is ignored, the model results provide the maximum limit of horizontal migration of the injected CO_2 (i.e., the actual horizontal spreading may be less when buoyancy is included). Thus these model predictions can be useful in conforming to point of compliance issues.

Figure 1 schematically shows the essential elements of the conceptual model. The storage formation is conceptualized as an infinite circular cylinder ($R_\infty \to \infty$), with a thickness of L. The origin of the coordinate system is located at the center in the bottom plane of the circular cylinder, as shown in Figure 1. CO_2 is injected through an injection borehole with radius r_w, which extends all the way to the ground surface. Note that the flow and transport processes inside the injection borehole are not explicitly modeled. As shown in Figure 1, the injection borehole is perforated between b_1 (the height of the bottom of the perforated zone measured from the origin) and b_2 (the height of the top of the perforated zone measured from the origin). The thickness of the perforated zone is thus $(b_2 - b_1)$, which is considerably smaller than the thickness of the storage formation, L. It is assumed that CO_2 enters the formation through the perforated zone at a mass flow rate of $\dot{m}$ (in units of kg s^{-1}) for a specified period of time, t_{inj}. No flow boundary conditions are applied at the top and bottom boundaries of the storage formation. At the radial boundaries (which are assumed to be located at a large distance from the injection borehole), constant pressure $(P = P_i)$ is assumed. It is also assumed that the injection process happens under isothermal conditions, that the storage formation was initially maintained at a uniform pressure of P_i, and that the storage formation has a horizontal permeability of k_r and a vertical permeability of k_z, with an anisotropy ratio of $\alpha = k_z / k_r$. Finally, because we are focusing on natural gas reservoirs, capillarity is excluded from the model.

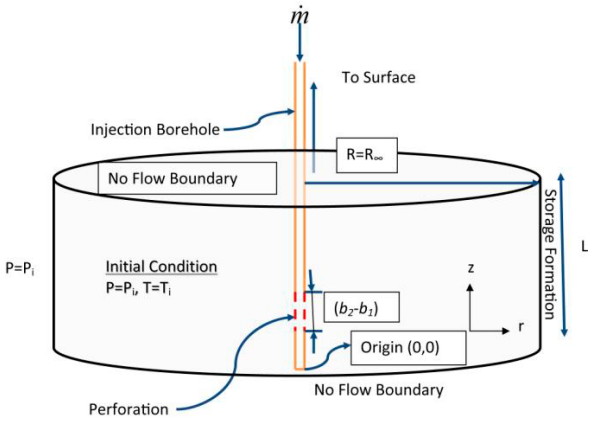

Figure 1. Schematic illustration of the conceptual model used for developing the analytical solution

3. Equation of State

For supercritical CO_2, it has been generally observed [6] that the correlations provided by Altunin [7] provide the best estimate of its physical properties. However, notwithstanding the accuracy of Altunin's correlations, they are difficult to use. In this paper, we instead begin with the generalized Pitzer correlations [8] as an alternative EOS for computing the physical properties of CO_2. To check the range of pressure over which Pitzer's correlations can be used, we show reduced volume (V_r) of CO_2 (ratio of volume of CO_2 and its critical volume V_c, i.e., $V_r = V/V_c$) as a function of pressure (P) in Figure 2. Note that the values of V_r were obtained from the CO2TAB file distributed with the TOUGH2/ECO2N software [6]. From Figure 2, we observe that, when T = 31.04°C, Pitzer's correlations can be used all the way up to the critical pressure (72.8 atm), beyond which V_r becomes smaller than 2.0, and the generalized Pitzer's correlations are no longer applicable [8]. However, as temperature is increased, Pitzer's correlations can be used even beyond the critical pressure.

Figure 3 shows the difference between the density calculated using Altunin's correlations (ρ) and that obtained from generalized Pitzer's correlations (ρ_P) as a function of pressure at different temperatures. We observe that the difference in density predicted by the two correlations increases approximately linearly over a large range of pressures, for pressures above the critical pressure. Based on this observation, we propose a relationship of the form

$$\rho - \rho_P = a(T) + b(T)P \tag{1}$$

where ρ is the density of supercritical CO_2 predicted by Altunin's correlations, ρ_P is the same predicted by Pitzer's correlations, P is pressure, and $a(T)$ and $b(T)$ are two temperature-dependent constants. The values of a and b at different temperatures can be found in [9]

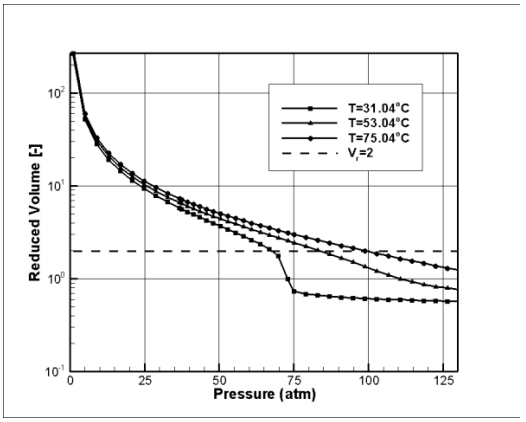

Figure 2. Reduced volume (V_r) of CO2 as a function of pressure at different temperatures

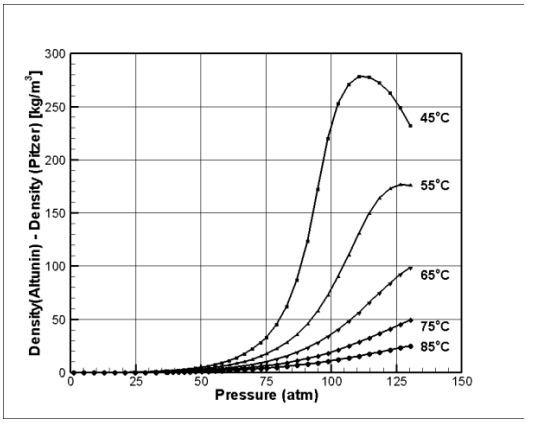

Figure 3: The difference in densities computed using Altunin's and gernalized Pitzer's correlations

4. Governing Equations and Boundary Conditions

Assuming Darcy flow regime, the differential equation describing flow of carbon dioxide in the storage formation under isothermal conditions can be written as

$$\frac{1}{r}\frac{\partial}{\partial r}\left(r\rho\frac{\partial P}{\partial r}\right)+\alpha\frac{\partial}{\partial z}\left(\rho\frac{\partial P}{\partial z}\right)=\frac{\phi\bar{\mu}}{k_r}\frac{\partial\rho}{\partial t} \tag{2}$$

where α is the anisotropy ratio. In writing Equation 2, we have assumed that the viscosity of carbon dioxide is constant over the pressure range typically encountered during injection in a gas reservoir. In Equation 2, ρ is the true density of CO_2 (as obtained from, say, Altunin's correlations), which is different from ρ_P — the Pitzer density (see Equation 1). By definition

$$\rho_P = \frac{PM}{ZRT} \tag{3}$$

where M is the molecular weight of CO_2, and $Z = 1 + BP/RT$ is the compressibility factor, and B is the second virial coefficient. Combining Equations 1, 2, and 3, we can write after some manipulations

$$\frac{1}{r}\frac{\partial}{\partial r}\left(r\left\{\frac{M-\psi}{\psi^2}+\frac{aB}{\psi^2}+\frac{bRT}{\psi}\left(\frac{M-\psi}{\psi^2}\right)\right\}\frac{\partial\psi}{\partial r}\right)+\alpha\frac{\partial}{\partial z}\left(\left\{\frac{M-\psi}{\psi^2}+\frac{aB}{\psi^2}+\frac{bRT}{\psi}\left(\frac{M-\psi}{\psi^2}\right)\right\}\frac{\partial\psi}{\partial z}\right)= \tag{4}$$

$$-\frac{\phi\bar{\mu}B}{MRTk_r}\frac{\partial}{\partial t}\left[(M-\psi)+aB+bRT\frac{M-\psi}{\psi}\right]$$

where $\psi = M - B\rho_P$. If we define $\theta = -\left[\frac{M}{\psi} + \ln\psi + \frac{(aB - bRT)}{\psi} + \frac{MbRT}{2\psi^2}\right]$, Equation 4 simplifies to

$$\frac{1}{r}\frac{\partial}{\partial r}\left(r\frac{\partial\theta}{\partial r}\right) + \alpha\frac{\partial}{\partial z}\left(\frac{\partial\theta}{\partial z}\right) = \frac{1}{\beta}\frac{\partial\theta}{\partial t} \tag{5}$$

where β (which has units of diffusivity, m^2/s) is defined as

$$\beta = \frac{k_r MRT}{\phi\bar{\mu}B}\left[\frac{\frac{M-\bar{\psi}}{\bar{\psi}^2} + \frac{aB}{\bar{\psi}^2} + \frac{bRT}{\bar{\psi}^3}(M-\bar{\psi})}{1 + \frac{MbRT}{\bar{\psi}^2}}\right] \tag{6}$$

One can obtain $\theta(r,z,t)$ by solving Equation 6. However, to be useful, we need to provide an expression for θ as a function of either pressure or density, which can be accomplished by using the Pitzer's correlations—the details of the derivation can be found in [9]

$$Ze^{-\left(C_1 Z + C_2 Z^2\right)} = Me^{\theta} \tag{7}$$

where $C_1 = 1 + \frac{aB}{M} - \frac{bRT}{M}$ and $C_2 = \frac{bRT}{2M}$. Thus, once θ is known from Equation 6, Z can be obtained by solving the nonlinear equation in Equation 7. $P(r,z,t)$ can then be obtained from $P(r,z,t) = \frac{RT}{B}[Z(r,z,t) - 1]$. The initial and boundary conditions are $P(r,z,0) = P_i$; $\frac{\partial P}{\partial z}\big|_{z=0} = 0$; $\frac{\partial P}{\partial z}\big|_{z=L} = 0$; $P(\infty,z,t) = P_i$, $2\pi r_w(b_2 - b_1)\frac{k_r}{\mu}\rho\frac{\partial P}{\partial r}\big|_{r=r_w} = \dot{m}F$, where $F = U(z-b_1) - U(z-b_2)$, and $U(z\text{-}a)$ is the unit step function.

5. Analytical Solution

To cast Equation 6 into dimensionless form, we define $\theta_D = \frac{\theta_i - \theta}{\theta_i}$, $\xi = \frac{r}{r_w}$, $\zeta = \frac{z}{r_w}$, and $\tau = \frac{\beta t}{r_w^2}$. Using these dimensionless variables, we rewrite Equation 6 as

$$\frac{1}{\xi}\frac{\partial}{\partial\xi}(\xi\theta_D) + \alpha\frac{\partial}{\partial\zeta}\left(\frac{\partial\theta_D}{\partial\zeta}\right) = \frac{\partial\theta_D}{\partial\tau} \tag{8}$$

The detailed procedure for solving Equation 8 is given in [9]. After taking a Fourier finite cosine transform of Equation 8 and then applying Laplace transform, we obtain

$$\frac{1}{\xi}\frac{d}{d\xi}\left(\xi\frac{d\hat{\bar{\theta}}_D}{d\xi}\right) = q_1^2\hat{\bar{\theta}}_D \tag{9}$$

where $q_1 = \sqrt{p + \alpha\omega_n^2}$, $\omega_n = \frac{n\pi}{L_D}$, and p is the Laplace parameter. The solution of Equation 9 can be written as [10]

$$\hat{\bar{\theta}}_D(\xi,\omega_n,p) = \frac{\dot{m}_D[\sin(\omega_n B_2) - \sin(\omega_n B_1)]}{\omega_n p q_1}\frac{K_0(q_1\xi)}{K_1(q_1)} \tag{10}$$

where $\dot{m}_D = \frac{\dot{m}}{2\pi(b_2 - b_1)\frac{k_r}{\mu}\theta_i\frac{MRT}{B^2}}$, $B_1 = \frac{b_1}{r_w}$, and $B_2 = \frac{b_2}{r_w}$.

Performing an inverse Fourier transform [10], we obtain the following in the Laplace transform space

$$\hat{\theta}_D(\xi,\zeta,p) = \frac{\dot{m}_D}{p\sqrt{p}}\frac{(B_2 - B_1)}{L_D}\frac{K_0\left(\xi\sqrt{p}\right)}{K_1\left(\sqrt{p}\right)} + \frac{2\dot{m}_D}{L_D}\sum_{n=1}^{\infty}\frac{K_0(q_1\xi)}{pq_1K_1(q_1)}\frac{[\sin(\omega_n B_2) - \sin(\omega_n B_1)]}{\omega_n}\cos(\omega_n\zeta) \tag{11}$$

where $L_D = L/r_w$. A solution in real-time space can now be constructed using the procedures elaborated in [10]. This solution is

$$\theta(\xi,\zeta,\tau)=\frac{2\dot{m}_D}{\pi L_D}\left[(B_2-B_1)f_{1D}(\xi,\tau)+2\sum_{n=1}^{\infty}f_{2D}(\xi,\tau)\frac{\sin(\omega_n B_2)-\sin(\omega_n B_1)}{\omega_n}\cos(\omega_n\zeta)\right] \tag{12}$$

where $f_{1D}(\xi,\tau)=\int_0^{\infty}\left(1-e^{-u^2\tau}\right)\frac{Y_0(\xi u)J_1(u)-J_0(\xi u)Y_1(u)}{Y_1^2(u)+J_1^2(u)}\frac{du}{u^2}$ and

$f_{2D}(\xi,\tau)=\int_0^{\infty}\left[1-e^{-\left(u^2+\alpha\omega_n^2\right)\tau}\right]\frac{Y_0(\xi u)J_1(u)-J_0(\xi u)Y_1(u)}{Y_1^2(u)+J_1^2(u)}\frac{du}{u^2+\alpha\omega_n^2}$.

6. Results and Discussion

We assume one million tons $\left(1\times10^9\,kg\right)$ of carbon dioxide is injected into the target formation over a period of four years, resulting in a uniform injection rate $(\dot{m})$ of 7.922 kg s^{-1}. The thickness of the target formation (L) is 100 m. The bottom of the perforated zone (b_1) is situated at 45 m, while the top of the perforated zone (b_2) is at 55 m, giving a perforation thickness of 10 m. The diameter of the injection borehole is 0.1 m. In dimensionless terms, these parameters are $L_D=1000$, $B_1=450$, $B_2=550$, and $B_2-B_1=100$. Injection occurs at 80 atm or 0.8104×10^7 Pa, which is also the initial pressure of the formation (P_i). The formation temperature is 328.15 K (55°C). Assuming a geothermal gradient of 0.03°C/m and a surface temperature of 20°C, this will translate to an injection depth of about 1167 m (~3800 ft).

Figure 4 shows the formation pressure at four different times as a function of distance when the formation permeability is 1×10^{-14} m^2, and the anisotropy ratio is unity. For this scenario, pressure reaches a maximum of about 12.8 MPa close to the injection borehole, and gradually declines as one moves away from the borehole. The impact of injection (in terms of pressure) can be experienced up to approximately one kilometer from the borehole. i.e., there will be minimal changes in pressure beyond one kilometer. Note that, because we have ignored buoyancy effects, the actual maximum pressure buildup near the borehole will be somewhat smaller than the estimated 12.8 MPa (as shown in Figure 4). The estimated pressure buildup at the borehole thus represents an upper limit. For the same reason (i.e., not including the buoyancy effects), the actual radial extent of the pressure change because of injection will be shorter than that shown in Figure 4.

The impact of permeability anisotropy on pressure buildup resulting from carbon dioxide injection is illustrated in Figures 5. Figure 6 shows pressure as a function of radial distance at one year for different anisotropy ratios. When α = 0.1, the injected CO_2 will have relatively more difficulty moving vertically as opposed to horizontally. Thus, at any specified time, more of the injected mass of CO_2 reaches a fixed radial location when α = 0.1 (compared to the situation when α = 1). Consequently, the increase in pressure at a fixed radial location at a specified time is more when α = 0.1 (compared to the situation when α = 1). This trend is expected to be even more pronounced when α is reduced further. The converse is true when vertical permeability is more than radial permeability, as illustrated by the plots for α = 10 and 100 in Figure 5. Because more CO_2 flows in the vertical direction relative to the radial direction, pressure buildup along the radial direction is relatively less severe (compared to the isotropic case).

One of the key factors influencing the extent of pressure buildup is the formation permeability. This is illustrated in Figures 6 and 7, which shows pressure as a function of radial distance at 1 year for three different radial permeabilities. When the formation is highly permeable (k_r = 1×10^{-13} m^2), there is an insignificant change in pressure. As permeability is reduced more and more, significant buildup in pressure happens, particularly close to the injection borehole. If an estimate of formation permeability is available before the start of carbon dioxide injection, Figure 6 can be used as a reference for determining the injection rate that will not result in buildup of pressure beyond allowable limits. Figure 7 shows essentially the same results as Figure 6, except it shows pressure as a function of time at a radial location of r = 10 m for three different radial permeabilities.

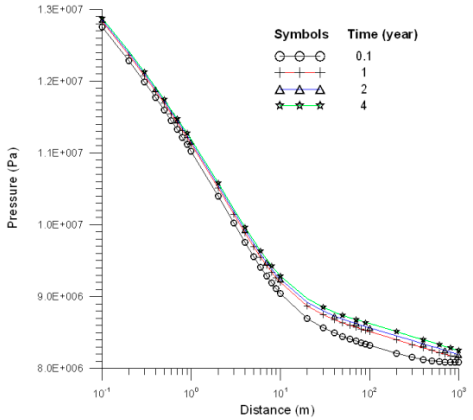

Figure 4. Pressure buildup as a function of radial distance at different times when formation anisotropy ratio is unity and permeability is 1×10^{-14} m^2

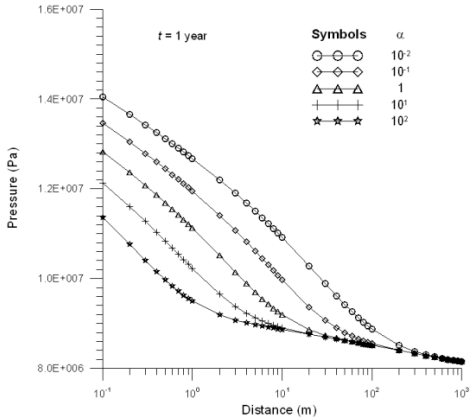

Figure 5. Pressure buildup as a function of radial distance with different anisotropy ratio at t = 1 year, when formation permeability is 1×10^{-14} m^2

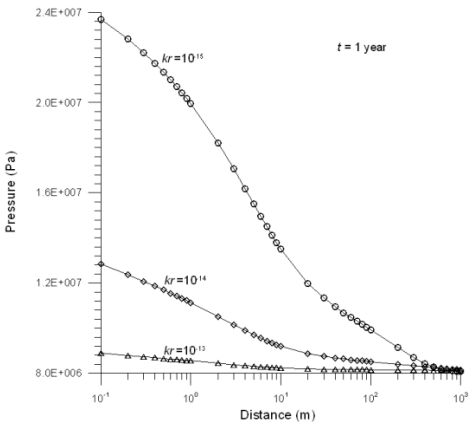

Figure 6. Pressure buildup as a function of radial distance at t =1 year with different formation horizontal permeabilities, when anisotropy ratio is unity

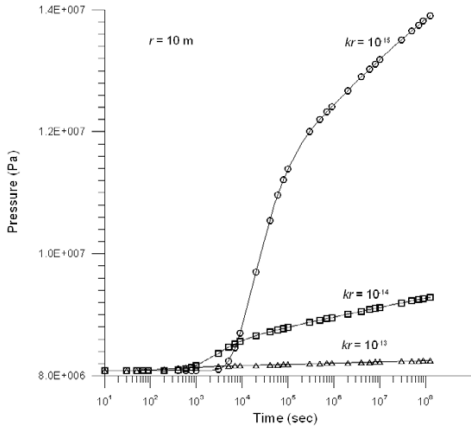

Figure 7. Pressure buildup as a function of time at r = 10 m with different formation horizontal permeabilities, when anisotropy ratio is unity

7. Summary

In this paper, we present an analytical solution for predicting the extent of pressure buildup resulting from CO_2 injection into a gas reservoir. This analytical solution is not formation specific, and is general in nature. It is also more appropriate than empirical relationships based on oil and gas operations. These analytical solutions can thus be used as guidelines for maximum injection rates without exceeding safe pressure limits, particularly when not much information is available about the storage formation. The storage formation is conceptualized as an infinite cylinder, which has a finite thickness, with the thickness of the perforated zone considerably smaller than the thickness of the formation. No flow conditions are applied at the top and bottom boundaries, and constant pressure condition is assumed at the radial boundaries. Injection happens under isothermal conditions and the storage formation is initially maintained at a uniform pressure. Permeabilities are assumed to be anisotropic, consistent with most subsurface storage formations. To obtain maximum limits on pressure buildup near the injection well or on the maximum extent of horizontal spreading, we exclude the effects of buoyancy. Supercritical CO_2 has a density similar to that of a liquid and a viscosity similar to that of a gas. An appropriate equation of state is needed to estimate the physical properties of supercritical CO_2. It has been generally concluded [6] that Altunin's correlations [7] provide the most accurate estimates of CO_2 physical properties. However, these correlations have complex

functional forms, making them difficult to use for analytical purposes. In this paper, we use Pitzer's correlations after introducing correction terms to make them consistent with Altunin's correlations. The differential equation controlling the spread of CO_2 after injection was obtained from mass-balance conditions. The solution to the differential equation was first obtained in the Fourier-Laplace space, and then inverted back to real space and time. Typical transient pressure buildup plots are shown for various formation permeabilities and anisotropy ratios.

Acknowledgments

The authors acknowledge the review comments from Daniel Hawkes and Guoping Lu of Berkeley Lab. Support is provided to Berkeley Lab through the U.S. Department of Energy Contract No. DE-AC02-05CH11231.

References

- [1] IPCC (Intergovernmental panel on Climate Change). IPCC Special Report on Carbon Dioxide Capture and Storage. New York: Cambridge University Press; 2005.
- [2] van der Meer, B. Carbon dioxide storage in natural gas reservoirs, Oil & gas Science and Technology – *Rev. IFP* 2005; 60:527-536.
- [3] Oldenburg, CM. Geologic carbon sequestration: CO_2 transport in depleted gas reservoirs. In: Ho, CK, Webb, SW, editors. Gas Transport in Porous Media, London, UK: Springer; 2006, pp. 419-426.
- [4] Li, Z, Dong, M, Li, S, and Huang, S. Sequestration in depleted oil and gas reservoirs – caprock characterization and storage capacity. Energy Conversion and Management 2006; 47:1372-1382.
- [5] Oldenburg, CM. Joule-Thomson cooling due to CO_2 injection into natural gas reservoirs. Energy Conversion and Management 2007; 48:1808-1815.
- [6] Pruess, K. ECO2N: A TOUGH2 fluid property module for mixtures of water, NaCl, and CO_2, Report LBNL-57952. Berkeley: Lawrence Berkeley National Laboratory; 2005.
- [7] Altunin, VV. Thermophysical Properties of Carbon Dioxide. Moscow, Russia: Publishing House of Standards; 1975.
- [8] Smith, JM and Van Ness, HC. Introduction to Chemical Engineering Thermodynamics. 3rd ed. New Delhi, India: McGraw-Hill; 1981.
- [9] Mukhopadhyay, S, Yang, SY, and Yeh, HD. An analytical solution for pressure buildup during supercritical carbon dioxide injection from a partially penetrating borehole into gas reservoirs. International Journal of Greenhouse Gas Control 2010; in review.
- [10] Yang, SY, Yeh, HD, and Chiu, PY. A closed form solution for constant flux pumping in a well under partial penetration condition. Water Resour. Res. 2006, W05502, doi:10.1029/2004WR003889.